

# Rapid preparation and magnetodielectric properties of trirutile $\text{Cr}_2\text{WO}_6$

Cite as: J. Appl. Phys. **117**, 014105 (2015); <https://doi.org/10.1063/1.4905486>

Submitted: 17 November 2014 . Accepted: 22 December 2014 . Published Online: 07 January 2015

 Michael W. Gaultois, Moureen C. Kemei, Jaye K. Harada, and Ram Seshadri



View Online



Export Citation



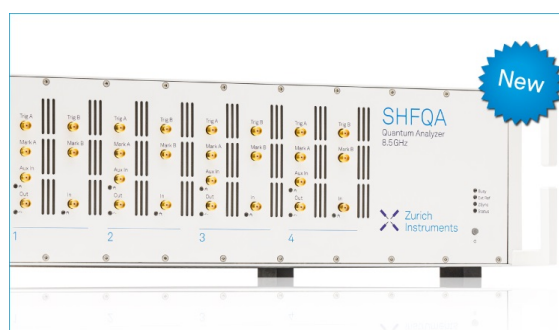
CrossMark

## ARTICLES YOU MAY BE INTERESTED IN

Manipulation of magnetic field on dielectric constant and electric polarization in  $\text{Cr}_2\text{WO}_6$   
Applied Physics Letters **104**, 132908 (2014); <https://doi.org/10.1063/1.4870518>

Structural, dielectric and magnetic studies of magnetoelectric trirutile  $\text{Fe}_2\text{TeO}_6$   
AIP Conference Proceedings **1731**, 130037 (2016); <https://doi.org/10.1063/1.4948143>

Structural, dielectric and magnetic studies of  $\text{Fe}_2\text{TeO}_6$  and  $\text{Fe}_2\text{Te}_{0.96}\text{Nb}_{0.04}\text{O}_6$  ceramics  
AIP Conference Proceedings **1832**, 140026 (2017); <https://doi.org/10.1063/1.4980808>



## Your Qubits. Measured.

Meet the next generation of quantum analyzers

- Readout for up to 64 qubits
- Operation at up to 8.5 GHz, mixer-calibration-free
- Signal optimization with minimal latency

Find out more



## Rapid preparation and magnetodielectric properties of trirutile $\text{Cr}_2\text{WO}_6$

 Michael W. Gaultois,<sup>1,2,a)</sup> Moureen C. Kemei,<sup>1</sup> Jaye K. Harada,<sup>1,3</sup> and Ram Seshadri<sup>1,2,3</sup>
<sup>1</sup>Materials Research Laboratory, University of California, Santa Barbara, California 93106, USA

<sup>2</sup>Department of Chemistry and Biochemistry, University of California, Santa Barbara, California 93106, USA

<sup>3</sup>Materials Department, University of California, Santa Barbara, California 93106, USA

(Received 17 November 2014; accepted 22 December 2014; published online 7 January 2015)

Dense pellets of >99% purity trirutile  $\text{Cr}_2\text{WO}_6$  were prepared in one step from starting oxides using spark plasma sintering, leading to simultaneous reaction and consolidation in 3 min at 1473 K. The reducing environment during processing may be partly responsible for the rapid reaction time in these oxides, with partial reduction of  $\text{Cr}^{3+}$  and the associated oxygen vacancies allowing rapid diffusion of cations. The low-temperature physical properties of  $\text{Cr}_2\text{WO}_6$  were examined, and a new transition at  $T = 5.9$  K was observed as an anomaly in the temperature-dependent dielectric permittivity and a corresponding anomaly in the specific heat. A strong enhancement of the magnetocapacitance is observed below this transition temperature at  $T = 5.9$  K and may be associated with a change from collinear spin order to more complex spin order. © 2015 AIP Publishing LLC. [<http://dx.doi.org/10.1063/1.4905486>]

### I. INTRODUCTION

The preparation of complex oxides with multiple metal ions frequently involves cycles of intimate grinding of the starting oxide powders and annealing at high temperatures in a process that can take multiple days. The long heating times are a consequence of the slow rate of solid-state diffusion for most ions in oxide environments. This is particularly true in the case of  $\text{Cr}_2\text{WO}_6$  (Refs. 1 and 2)—the compound of interest here—as  $\text{Cr}_2\text{O}_3$  is quite inert and diffuses rather slowly, a property that is responsible for its protective properties as one of the primary protective oxides in engineering materials, such as steels. There are frequently other complications as well. Notably for this material class,  $\text{WO}_3$  is a volatile solid, making it challenging to obtain single-phase materials using the extended reaction times required to enable  $\text{Cr}^{3+}$  mobility. Moreover, the resulting materials after traditional solid state reaction are powders or low density sintered bodies that require consolidation and/or densification to achieve dense bodies suitable for physical property measurement. This can be accomplished by hot-pressing at elevated temperatures for extended times (generally several hours), though this introduces further challenges, including the potential for decomposition, or, in this case, volatilization.

This contribution describes the use of spark plasma sintering (SPS), more accurately described as current-assisted, pressure-activated densification (CAPAD),<sup>3</sup> to rapidly prepare multi-gram quantities of high purity, dense samples of  $\text{Cr}_2\text{WO}_6$  in a single processing step that takes less than an hour. The rapid processing times and simultaneous reaction and consolidation overcome many of the common pitfalls of traditional ceramic methods. Further, we describe how the rapid reaction times allowed by this processing (<3 min at 1473 K for  $\text{Cr}_2\text{WO}_6$ ) may be related to fundamental rates of well-understood models of ligand exchange in aqueous molecular metal complexes.

$\text{Cr}_2\text{WO}_6$  was prepared and studied here as a candidate magnetodielectric material.  $\text{Cr}_2\text{WO}_6$  adopts an inverse trirutile-type crystal structure (Figure 1) and was proposed to have potential magnetodielectric properties by Hornreich,<sup>4</sup> and more recent work has investigated the magnetoelectric coupling in  $\text{Cr}_2\text{WO}_6$  near the antiferromagnetic ordering temperature at  $\sim 45$  K.<sup>5</sup> The coupling of magnetic and electric properties is of great interest for next generation information storage, where an electric field may control and interrogate the magnetic state of a memory storage device. Complete characterization of magnetodielectric materials is imperative to

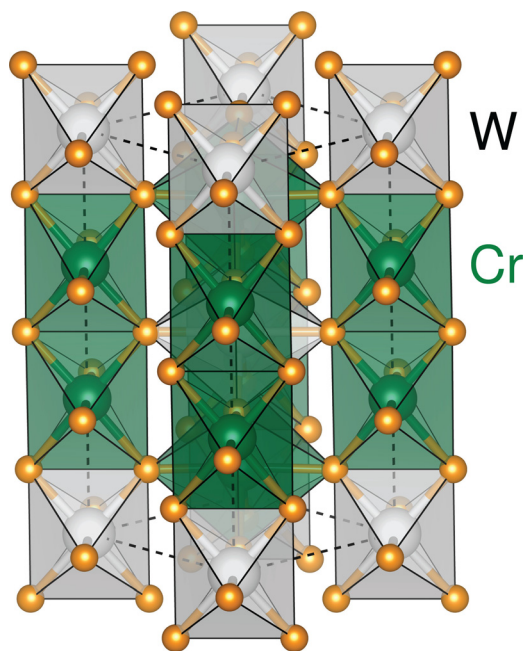


FIG. 1.  $\text{Cr}_2\text{WO}_6$  adopts the inverse trirutile structure ( $P4_2/mnm$ , 136), which consists of parallel columns of edge-sharing  $\text{MO}_6$  ( $M = \text{Cr}, \text{W}$ ) octahedra extending along the  $c$ -axis.  $\text{Cr}^{3+}$  atoms are shown in green, and  $\text{W}^{6+}$  in white. These columns are connected through O at the corners of the edge-sharing octahedra.

<sup>a)</sup>Electronic mail: mgaultois@mrl.ucsb.edu.

understand the complex interaction of magnetism and dielectric polarization. This report presents the low-temperature physical properties of  $\text{Cr}_2\text{WO}_6$  and reveals a new transition at  $T = 5.9\text{ K}$  observed by changes in the dielectric permittivity and specific heat. This is keeping with other recent studies that have revealed dielectric permittivity and magnetocapacitance measurements are sensitive probes of subtle changes in magnetic/crystal structure accompanying magnetic ordering, as well as changes in magnetic symmetry.<sup>6,7</sup>

## II. EXPERIMENTAL DETAILS

Polycrystalline samples were made by reaction and consolidation of binary oxide powders ( $\text{WO}_3$ , 99.9%, Sigma-Aldrich;  $\text{Cr}_2\text{O}_3$ , 99.99%, Sigma-Aldrich) using spark plasma sintering on an instrument from FCT Systeme GmbH, Germany. In a chamber base pressure of 10 Torr of argon, 80 MPa uniaxial pressure was applied using a 9 mm inner-diameter graphite die (EDM-4, POCO graphite). The sample was then heated rapidly to 1473 K at 200 K/min, annealed for 3 min at 1473 K, then rapidly cooled at 200 K/min (Figure 2). During the SPS annealing step, 5.0 V and 980 A were applied across the die set. X-ray diffraction (XRD) was performed on the pellet using a laboratory instrument (Philips X'Pert diffractometer,  $\text{Cu K}\alpha$  radiation), and diffractograms were consistent with single-phase  $\text{Cr}_2\text{WO}_6$ ; no secondary phases were observed. When ground, the resulting  $\text{Cr}_2\text{WO}_6$  powder is brown in colour. The conditions in SPS processing are highly reducing (elevated temperatures in a graphite die in low pressures of argon), so pellets were subsequently annealed in air to ensure full oxygen stoichiometry and minimize defects. Pellets were annealed in air at 1273 K for 24 h and cooled to room temperature at 2 K/min. Reaction with  $\text{Al}_2\text{O}_3$  or  $\text{SiO}_2$  is problematic, so pellets were annealed on a bed of sacrificial  $\text{Cr}_2\text{WO}_6$  powder. Annealed

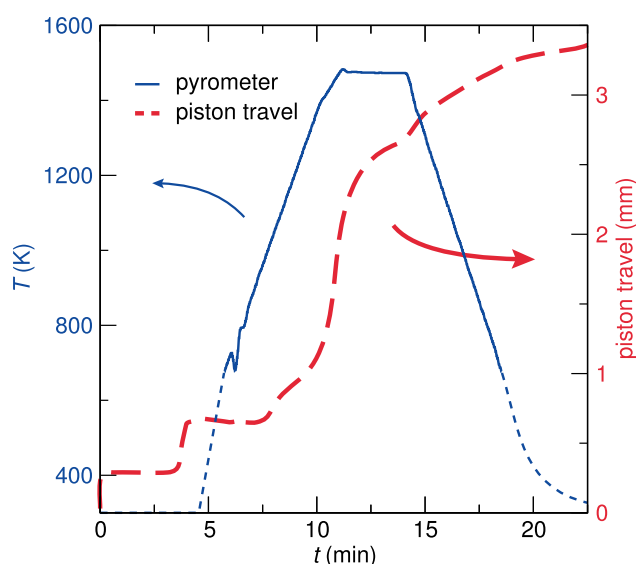


FIG. 2. SPS can be used to prepare dense pellets of  $\text{Cr}_2\text{WO}_6$  from a mixture of binary oxides ( $\text{Cr}_2\text{O}_3 + \text{WO}_3$ ) in under 30 min total. 80 MPa of uniaxial pressure was applied and the sample was heated rapidly from 673 K to 1473 K at 200 K/min, annealed for 3 min at 1473 K, then rapidly cooled at 200 K/min. The temperature profile below 673 K is estimated, as the pyrometer is unreliable below 673 K.

pellets had a density of  $6.74\text{ g/cm}^3$  to  $6.77\text{ g/cm}^3$  (99% single crystal density), measured by He pycnometry using a MicroMeritics AccuPyc 1340 Pycnometer. Annealed material was used for all experimental measurements reported here; synchrotron XRD of annealed material revealed a 0.7(1) mol. %  $\text{Cr}_2\text{O}_3$  impurity that was not observed by lab XRD because of the lower sensitivity of the lab instrument.

High-resolution synchrotron XRD data on finely ground powder was acquired at 295 K at beamline 11-BM at the Advanced Photon Source, Argonne National Laboratory, using an average wavelength of  $0.413682\text{ \AA}$  on a diffractometer that has been described in detail by Wang *et al.*<sup>8</sup> The precise wavelength was determined using a mixture of Si (SRM 640 c) and  $\text{Al}_2\text{O}_3$  (SRM 676) NIST standards run in a separate measurement. Samples were contained in 0.8 mm diameter Kapton capillaries and the packing density was low enough that absorption was not noticeable. Rietveld refinement was performed using TOPAS 5 Academic<sup>9</sup> and verified using GSAS-II.<sup>10</sup> Instrument profile parameters were determined using Si (SRM 640 c) and  $\text{LaB}_6$  (SRM 660 b) NIST lineshape standards, run in separate measurements. The refined lattice parameters of  $\text{Cr}_2\text{WO}_6$  were  $a = 4.579269(4)\text{ \AA}$  and  $c = 8.66328(9)\text{ \AA}$ .

Magnetic properties of powders were measured using a Quantum Design Dynacool vibrating sample magnetometer (VSM). Zero-field cooled (ZFC) and field cooled cooling (FCC) measurements were performed between 2 K and 380 K with 1000 Oe applied dc magnetic field. ZFC–FCC data were collected while heating (ZFC) or cooling (FCC) at 1 K/min, while the field-dependent susceptibility was collected while sweeping the magnetic field at 100 Oe/s. Low-temperature heat capacity was measured using a Quantum Design Physical Properties Measurement System (PPMS). Heat capacity measurements were performed on a pellet of mass 32.72 mg cut from the SPS-densified material and analyzed using the thermal relaxation dual-slope method. A thin layer of Apiezon N grease ensured thermal contact between the platform and the sample. The heat capacity of the Apiezon N grease was collected separately and subtracted from the measured sample heat capacity.

Dielectric properties were measured by an Andeen-Hagerling AH2700A capacitance bridge connected to the sample by shielded coaxial cables. A dense cylindrical sample (9.57 mm diameter, 1.41 mm thick, 99% apparent density) was placed in a Quantum Design Dynacool PPMS, which provides control of the temperature and field when carrying out dielectric measurements. To confirm the minor  $\text{Cr}_2\text{O}_3$  impurity (0.7 mol. %) did not influence the capacitance, additional measurements were conducted on a single-phase  $\text{Cr}_2\text{O}_3$  pellet (prepared by the same process conditions described above), and these measurements confirm the lack of similar features in the temperature- and field-dependent capacitance.

## III. RESULTS AND DISCUSSION

### A. Rapid preparation of single-phase material

SPS offers a rapid preparatory route to prepare dense, single-phase material in a single processing step that takes

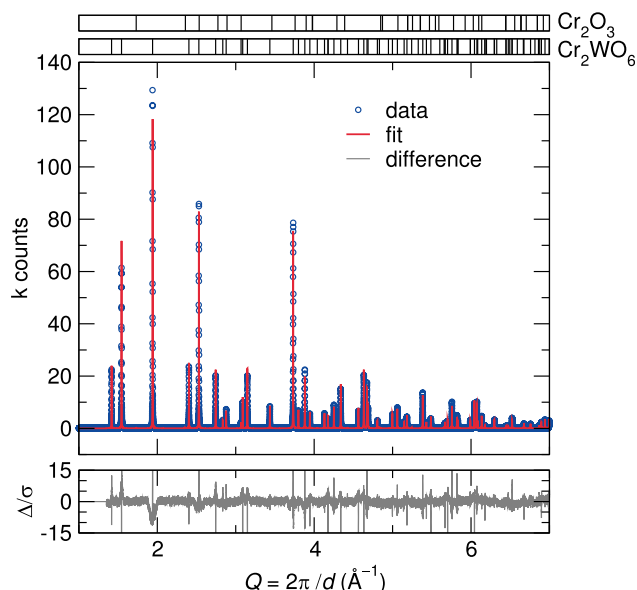


FIG. 3. Rietveld analysis of synchrotron powder X-ray diffraction data reveals this particular sample contains 99.3(1) mol. %  $\text{Cr}_2\text{WO}_6$ , with a 0.7(1) mol. %  $\text{Cr}_2\text{O}_3$  secondary phase, though this minor impurity does not affect the bulk properties in this report. This sample was prepared using SPS from a mixture of binary oxides ( $\text{Cr}_2\text{O}_3 + \text{WO}_3$ ) in 3 minutes at 1473 K.

$\sim 30$  min total (including cool-down). SPS led to dense pellets of  $\text{Cr}_2\text{WO}_6$  with  $> 99\%$  phase purity (Figure 3). We have previously observed that extremely high pellet densities are essential for high quality dielectric data. Reaction times to achieve phase-pure materials were as short as 3 min at the reaction temperature (1473 K), the shortest time attempted (Figure 2). Solid state reactions generally take several days, and the reaction rates are generally limited by diffusion. Although no hard rule set exists to determine the reaction rate of solid metal oxides, we propose the extensive studies of molecular metal aqua complexes may provide useful guidelines.

$\text{Cr}^{3+}$  ( $d^3$ ) is notoriously inert due to the large crystal field stabilization energy provided by a half-filled  $t_{2g}^3$  level in an octahedral coordination geometry (Figure 4).<sup>11</sup> This leads

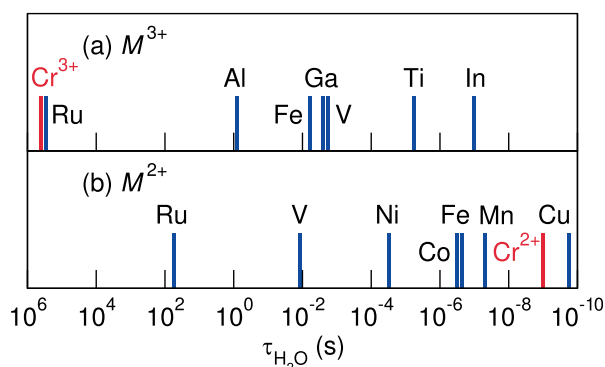


FIG. 4. The mean residence time of water molecules in metal hexaqua complexes may be a useful proxy to understand solid state reactions of oxides. Inert cations, such as  $\text{Cr}^{3+}$ , lie on the left, while reactive cations with labile ligands lie towards the right, such as  $\text{Cr}^{2+}$ . While ions of lower charge/radius ratio are expected to react more quickly (for example, the series of  $\text{Al}^{3+}$ ,  $\text{Ga}^{3+}$ , and  $\text{In}^{3+}$ ), the crystal field stabilization energy dominates the reactivity of transition metal ions. The reducing conditions in SPS processing may lead to partial reduction of  $\text{Cr}^{3+}$  and creation of oxygen vacancies, and may explain the unexpectedly rapid reaction times possible with SPS ( $< 3$  min). Data from Ref. 11.

to a stable coordination shell with an extremely long mean residence time of water molecules in the  $[\text{Cr}(\text{H}_2\text{O})_6]^{3+}$  complexes ( $\sim 5$  days), compared to the blindingly fast residence time in  $\text{Cr}^{2+}$  hexaqua complexes ( $\sim 10^{-9}$  s). In solid Cr oxides, the  $\text{CrO}_6$  octahedral coordination shell is expected to be inert, and lead to slow diffusion of  $\text{Cr}^{3+}$  cations. The unexpectedly short reaction times for  $\text{Cr}_2\text{WO}_6$  using SPS may result from partial reduction of  $\text{Cr}^{3+}$  and oxygen vacancies created by the reducing conditions during SPS processing. Creation of  $\text{Cr}^{2+}$  would lead to much more labile oxide anions, and disordered oxygen vacancies would be expected to decrease the activation energy barrier associated with interstitial or vacancy hopping diffusion of Cr species, thus increasing the rate of diffusion and decreasing the reaction time between powdered metal oxide precursors.

The reducing conditions during SPS undoubtedly lead to partial reduction of  $\text{WO}_3$ , though this alone is insufficient to lead to the rapid reaction times reported here. Attempts to produce pseudobinary  $\text{Al}_2\text{O}_3\text{--WO}_3$  phases under similar SPS conditions resulted in only minor product formation and the recovery of starting materials, as determined by lab XRD. This is consistent with our suggested model, as  $\text{Al}^{3+}$  is expected to be much more inert than  $\text{Cr}^{2+}$  (Figure 4;  $\tau_{\text{Al}^{3+}} \approx 10^9 \tau_{\text{Cr}^{2+}}$ ), and  $\text{Al}^{3+}$  is not expected to reduce as easily as  $\text{Cr}^{3+}$  ( $\text{Cr}^{3+} + e^- \leftrightarrow \text{Cr}^{2+}$ ,  $E^\circ = -0.4$  V;  $\text{Al}^{3+} + 3e^- \leftrightarrow \text{Al}$ ,  $E^\circ = -1.7$  V).<sup>12</sup>

Because of the reduction during SPS processing, thin pellets (thickness  $\sim 1$  mm) were annealed to ensure full oxygen stoichiometry before measuring physical properties. Annealing of powders or pellets resulted in no statistically significant change in lattice parameter detectable by laboratory XRD, and the appearance of the annealed powder is brown and indistinguishable from samples before annealing. Further, the effective moment extracted from the bulk magnetic susceptibility agrees with the calculated spin-only value for  $\text{Cr}_2\text{WO}_6$  (see below), suggesting there are no extra spins that might be present due to partially reduced metal centres. Annealed material was used for all experimental measurements reported here.

## B. Magnetic and electrical properties

Complex magnetic interactions arise in the trirutile-type structures because of the unique connectivity in the crystal structure: parallel columns of edge-sharing  $\text{MO}_6$  ( $M = \text{Cr}, \text{W}$ ) octahedra extending along the  $c$ -axis (Figure 1). Systematic studies performed by Yamaguchi and Ishikawa have examined the nature of the magnetic phenomena associated with several members of this structural family, including  $\text{Cr}_2\text{WO}_6$ .<sup>13</sup> Low-dimensional, short-range antiferromagnetic correlations give rise to a broad maximum in the magnetic susceptibility [(Figure 5(a)), which Yamaguchi and Ishikawa quantitatively describe using an anisotropic 2D Heisenberg model.<sup>13</sup> Long-range 3D antiferromagnetic order takes place at  $T_N \approx 45$  K,<sup>2</sup> which is more easily seen in the heat capacity (Figure 6).

The higher-temperature region (300 K to 370 K) of the ZFC inverse susceptibility was fit to the Curie–Weiss (CW) equation,  $\chi = C/(T - \Theta_{\text{CW}})$  to extract a Weiss temperature of  $\Theta_{\text{CW}} = -191$  K [Figure 5(b)], which is consistent with previous reports of  $-189$  K.<sup>13</sup> An effective moment of

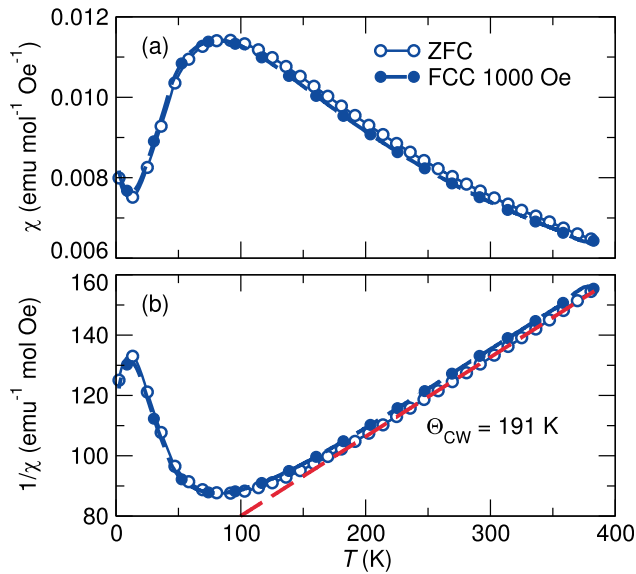


FIG. 5. (a) Magnetic susceptibility and (b) inverse susceptibility of  $\text{Cr}_2\text{WO}_6$  (acquired at  $\sim 0.1$  K intervals). A Curie-Weiss fit to the ZFC magnetic susceptibility from 300 K to 370 K leads to a  $\Theta_{\text{CW}} = -191$  K. There is a slight offset between the ZFC and FCC curves at high temperature, likely due to a temperature lag.

$\mu_{\text{eff}} = 5.44 \mu_{\text{B}}$  per  $\text{Cr}_2\text{WO}_6$  formula unit was extracted using the relationship  $\mu_{\text{eff}}^2 = 3Ck_{\text{B}}/N$ , where  $C$  is the Curie constant from the CW equation. The  $\mu_{\text{eff}}$  is close to the calculated spin-only value of  $\mu_{\text{S}} = 5.48 \mu_{\text{B}}$ , and significantly less than the calculated unquenched  $\mu_{\text{L+S}}$  of  $7.35 \mu_{\text{B}}$ . Finally, the large negative Weiss temperature is much larger than the antiferromagnetic ordering temperature, which is characteristic of frustrated spin systems. Moderately frustrated systems tend to have a frustration index  $f \geq 3$ ,<sup>14</sup> a criterion that is satisfied for  $\text{Cr}_2\text{WO}_6$ , where  $f = 4.3$ .

Measuring the dielectric permittivity down to 2 K reveals a feature at  $T_{\text{N}} \approx 45$  K due to a known antiferromagnetic ordering transition, as well as a feature at  $T \approx 6$  K. Corresponding features in the specific heat are observed for

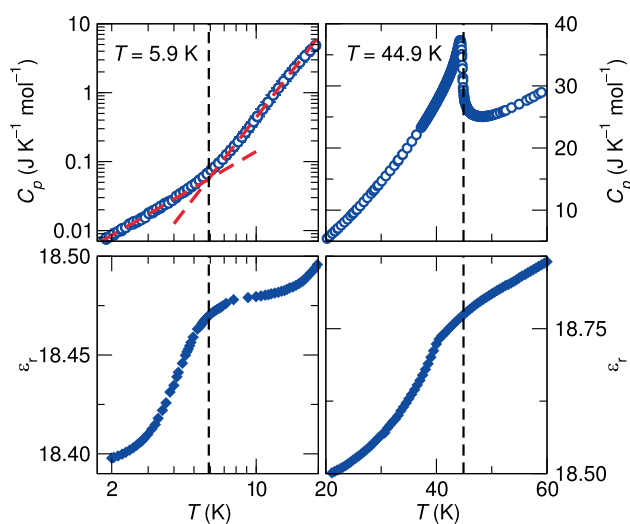


FIG. 6. Two transitions are observed by specific heat and dielectric permittivity as the temperature is decreased. The onset of the sharp change in the dielectric permittivity at  $T \approx 6$  K corresponds to a change in slope of the log-log specific heat.

both features, with a sharp  $\lambda$ -type anomaly at  $T_{\text{N}} = 44.9$  K, and a change in slope of the log-log specific heat at  $T = 5.9$  K (Figure 6). The transition temperature of  $T = 5.9$  K reported here is the intersection of linear fits to the log-log specific heat carried out on the linear regimes above and below the transition (Figure 6). ( $1.8$  K to  $4.0$  K:  $C_p = 2.54 \times 10^{-3} T^{1.74}$ ;  $9.0$  K to  $16.0$  K:  $C_p = 5.78 \times 10^{-5} T^{3.88}$ ) The values of the specific heat near  $T_{\text{N}} = 44.9$  K are consistent with a previous report from Yamaguchi *et al.*<sup>13</sup>

The nature of the transition at  $T = 5.9$  K was probed using field-dependent dielectric measurements in 3 key temperature regimes (Figure 7). Above the magnetic ordering temperature  $T_{\text{N}} \approx 45$  K, there is a weak, continuous increase of the dielectric permittivity with increasing applied magnetic field. Below 45 K, a local minimum in the field-dependence occurs at zero field, with weak local maxima at moderate applied fields ( $\sim 20$  kOe). Finally, below 6 K, in the region where a strong change is observed in the temperature-dependent dielectric permittivity, there is a strong enhancement in the magnetocapacitance response and the maxima shift to slightly higher field strength ( $\sim 35$  kOe). Compared to the magnetocapacitance at 35 K, the response at 2 K is enhanced by a factor of 400. The close correspondence of behavioural changes with known spin ordering and features in specific heat suggest these changes are intrinsic to  $\text{Cr}_2\text{WO}_6$  and not due to extrinsic resistive magnetocapacitance through a Maxwell-Wagner mechanism involving depleted grain boundaries.<sup>15</sup>

These regimes are analogous to behaviour seen in the field-dependent magnetization. The field-dependent

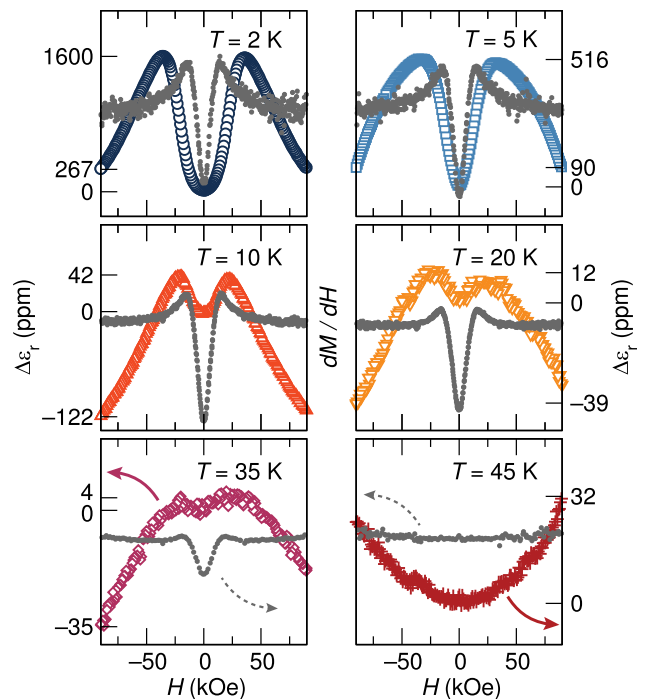


FIG. 7. Magnetocapacitance measurements show 3 temperature regimes:  $T > 45$  K,  $6 \text{ K} < T < 45$  K, and  $T < 6$  K. The magnetodielectric response changes upon magnetic ordering at  $T_{\text{N}} \approx 45$  K, and is strongly enhanced upon the lower-temperature transition at  $T \approx 6$  K. Compared to the magnetocapacitance at 35 K, the response at 2 K is enhanced by a factor of 400. Corresponding regimes are seen in the field-dependent magnetization, whose derivative is shown above (grey).

magnetization is consistent with paramagnetism above  $T_N \approx 45$  K and below the magnetic ordering temperature the magnetization shows small changes in slope at magnetic fields corresponding to the local extrema in the dielectric permittivity visible by magnetocapacitance. These changes are seen more readily in the derivative of the magnetization curves (Figure 7).

The sharp change in dielectric constant and strong enhancement of the magnetocapacitance below 6 K may be associated with a change from a collinear spin structure to more complex spin order, such as conical ordering.<sup>16–20</sup> Noncollinear spin ordering is common in magnetically frustrated systems, so this is not altogether unexpected here, since some frustration was noted ( $f=4.3$ ). Although the previous magnetic structure determination by Kunnmann *et al.* using neutron scattering at 4.2 K assigned a collinear magnetic structure,<sup>2</sup> most of the change in the dielectric permittivity has not yet taken place by 4.2 K (Figure 6) and is not complete until below 2 K. Other neutron scattering studies at 4.2 K observed extra weak reflections that could not be adequately described by a collinear spin structure, and were attributed to magnetostructural distortion, specifically, displacement of Cr ions.<sup>21</sup> This subtle magnetostructural distortion may be associated with changes in spin ordering, as has been demonstrated in recent reports of frustrated spinel oxides.<sup>7,22</sup> More detailed high-resolution neutron scattering studies at lower temperature may confirm this change in spin ordering.

The change in spin-order and the magnetostructural distortion would both be expected to contribute to the large change in dielectric permittivity reported here, and the magnetostructural distortion may be necessary for this to occur. The undistorted crystal structure symmetry of  $\text{Cr}_2\text{WO}_6$  ( $P4_2/mnm$ , 136;  $D_{4h}^{14}$ ) does not allow for any noncollinear spin structures, and Dzyaloshinskii-Moriya (DM) antisymmetric exchange between nearest neighbour Cr ions is not allowed because of the inversion centre at the midpoint (Wyckoff site  $2b$ , symmetry  $m.mm$ ). However, displacement of Cr ions through magnetostructural distortion will lower the symmetry of the crystal structure. This will likely break the inversion symmetry to allow for DM interactions, which may lead to canting of spins and a noncollinear spin structure, both of which would become more pronounced at lower temperature. This would lead to minimal changes to the entropy and gradual changes to the neutron diffraction but large changes to the dielectric response, as reported here.

#### IV. CONCLUSION

Dense pellets of >99% purity trirutile  $\text{Cr}_2\text{WO}_6$  were prepared by SPS, which led to simultaneous reaction and densification of  $\text{WO}_3$  and  $\text{Cr}_2\text{O}_3$  powders in 3 min at 1473 K. SPS offers a rapid route to prepare multi-gram quantities of high-purity, consolidated, dense materials that are in a suitable form for physical property measurement. The rapid processing times are ideally suited for materials that are volatile, such as  $\text{WO}_3$ . The reducing environment during processing may be partly responsible for the rapid reaction time in these oxides, where partial reduction of  $\text{Cr}^{3+}$  and creation of oxygen vacancies may allow rapid diffusion of cations.

The low-temperature physical properties of  $\text{Cr}_2\text{WO}_6$  were examined, and a new transition at  $T=5.9$  K was observed as an anomaly in the temperature-dependent dielectric permittivity and a corresponding anomaly in the specific heat. Below 6 K, a strong enhancement of the magnetocapacitance is observed and may be associated with magnetostructural distortion and/or a change from collinear spin order to more complex spin order.

#### ACKNOWLEDGMENTS

We thank the National Science Foundation for support of this research through NSF-DMR 1121053. M.W.G. thanks the Natural Sciences and Engineering Council of Canada for support through a Postgraduate Scholarship, and the U.S. Department of State for support through an International Fulbright Science & Technology Award. MWG thanks Stephen Wilson and Harlyn Silverstein for helpful discussions. M.C.K. thanks the Schlumberger Foundation for support through a Faculty for the Future award. The research carried out here made extensive use of shared experimental facilities of the Materials Research Laboratory: an NSF MRSEC, supported by NSF-DMR 1121053. The M.R.L. is a member of the the NSF-supported Materials Research Facilities Network ([www.mrfn.org](http://www.mrfn.org)). Use of data from beamline 11-BM at the Advanced Photon Source is supported by the Department of Energy, Office of Science, Office of Basic Energy Sciences, under Contract No. DE-AC02-06CH11357.

<sup>1</sup>M. C. Montmorey, E. F. Bertaut, and P. Mollard, *Solid State Commun.* **4**, 249 (1966).

<sup>2</sup>W. Kunnmann, S. Laplaca, L. M. Corliss, J. M. Hastings, and E. Banks, *J. Phys. Chem. Solids* **29**, 1359 (1968).

<sup>3</sup>J. E. Garay, *Annu. Rev. Mater. Res.* **40**, 445 (2010).

<sup>4</sup>R. M. Hornreich, *Solid State Commun.* **7**, 1081 (1969).

<sup>5</sup>Y. Fang, L. Y. Wang, Y. Q. Song, T. Tang, D. H. Wang, and Y. W. Du, *Appl. Phys. Lett.* **104**, 132908 (4pp) (2014).

<sup>6</sup>T. D. Sparks, M. C. Kemei, P. T. Barton, R. Seshadri, E.-D. Mun, and V. S. Zapf, *Phys. Rev. B* **89**, 024405 (6pp) (2014).

<sup>7</sup>P. T. Barton, M. C. Kemei, M. W. Gaultois, S. L. Moffitt, L. E. Darago, R. Seshadri, M. R. Suchomel, and B. C. Melot, *Phys. Rev. B* **90**, 064105 (7pp) (2014).

<sup>8</sup>J. Wang, B. H. Toby, P. L. Lee, L. Ribaud, S. M. Antao, C. Kurtz, M. Ramanathan, R. B. Von Dreele, and M. A. Beno, *Rev. Sci. Instrum.* **79**, 085105 (7pp) (2008).

<sup>9</sup>A. A. Coelho, "TOPAS Academic V5," (2013).

<sup>10</sup>B. H. Toby and R. B. Von Dreele, *J. Appl. Crystallogr.* **46**, 544 (2013).

<sup>11</sup>L. Helm, G. M. Nicolle, and A. E. Merbach, *Adv. Inorg. Chem.* **57**, 327 (2005).

<sup>12</sup>*CRC Handbook of Chemistry and Physics*, edited by W. Haynes, 93rd ed. (CRC Press, Boca Raton, FL, 2012).

<sup>13</sup>M. Yamaguchi and M. Ishikawa, *J. Phys. Soc. Jpn.* **63**, 1666 (1994).

<sup>14</sup>A. P. Ramirez, *Annu. Rev. Mater. Sci.* **24**, 453 (1994).

<sup>15</sup>G. Catalan, *Appl. Phys. Lett.* **88**, 102902 (6pp) (2006).

<sup>16</sup>T. Kimura, T. Goto, H. Shintani, K. Ishizaka, T. Arima, and Y. Tokura, *Nature* **426**, 55 (2003).

<sup>17</sup>G. Lawes, B. Melot, K. Page, C. Ederer, M. A. Hayward, T. Proffen, and R. Seshadri, *Phys. Rev. B* **74**, 024413 (2006).

<sup>18</sup>R. Tackett, G. Lawes, B. C. Melot, M. Grossman, E. S. Toberer, and R. Seshadri, *Phys. Rev. B* **76**, 024409 (6pp) (2007).

<sup>19</sup>T. Kimura and Y. Tokura, *J. Phys.: Condens. Matter* **20**, 434204 (2008).

<sup>20</sup>N. Mufti, A. A. Nugroho, G. R. Blake, and T. T. M. Palstra, *J. Phys.: Condens. Matter* **22**, 075902 (6pp) (2010).

<sup>21</sup>M. C. Montmorey and R. Newnham, *Solid State Commun.* **6**, 323 (1968).

<sup>22</sup>M. C. Kemei, J. K. Harada, R. Seshadri, and M. R. Suchomel, *Phys. Rev. B* **90**, 064418 (8pp) (2014).